Acta Oceanol. Sin., 2023, Vol. 42, No. 5, P. 102–116
https://doi.org/10.1007/s13131-022-2062-9
http://www.aosocean.com
E-mail: ocean2@hyxb.org.cn

Petrographical and mineral chemistry evidence to delineate the source/sources of the Central Indian Ocean Basin pumices

Niyati G. Kalangutkar[1]*, Sridhar D. Iyer[2]

[1] School of Earth, Ocean and Atmospheric Sciences, Goa University, Taleigao Plateau, Goa 403206, India

[2] Formerly with CSIR-National Institute of Oceanography, Dona Paula, Goa 403004, India

Received 16 July 2021; accepted 27 June 2022

Abstract

We present data pertaining to mineral assemblages and composition of the Central Indian Ocean Basin (CIOB) pumices. Eight groups of pumices were identified considering the presence of phenocrysts of plagioclase, clinopyroxene, orthopyroxene, hornblende and biotite together with the occurrence of quartz and glass. Pigeonite, fayalite and ulvospinelare reported for the first time from these pumices. In the eight groups, the modal percentage of the constituents are phenocrysts 3% to 19% (avg 9.6%), silicic glass 33% to 54% (avg 43%) and the rest is vesicles. Based on the above factors we have identified the possible sources of the CIOB pumices. The mineral compositions of plagioclase, pyroxenes, and biotite of the CIOB pumices were compared with those of Krakatau and Toba. Most of the plagioclase and pyroxene compositions resemble the Haranggoal Dacite Tuff of Toba and Krakatau. Considering the mineral assemblages and compositions, there are pumices which do not correlate to any of the above eruptions and are probably from yet unidentified source/sources. These sources could either be from nearby terrestrial volcanoes or intraplate seamounts present in the CIOB. In a global context, it is viable that petrological characteristics could be used as initial criteria to determine the source of pumices that occur at abyssal depths in the world ocean.

Key words: CIOB, pumice, petrography, mineral chemistry, Indonesian Arc, intraplate volcanism

Citation: Kalangutkar Niyati G., Iyer Sridhar D.. 2023. Petrographical and mineral chemistry evidence to delineate the source/sources of the Central Indian Ocean Basin pumices. Acta Oceanologica Sinica, 42(5): 102–116, doi: 10.1007/s13131-022-2062-9

1 Introduction

Pumices have a low specific gravity and their dispersal around a volcanic region is strongly controlled by prevailing winds, topography, ocean currents and sub-bottom bathymetry. Because of these factors the pumice fall deposits would be dispersed in different directions in contrast to pyroclastic flows and remobilised deposits (Sigurdsson et al., 1980). Based on an extensive study carried out on thousands of pumice clasts, Iyer and Sudhakar (1993) suggested the existence of a 600 000 km^2 of pumice field to be present in the Central Indian Ocean Basin (CIOB). A few of the CIOB pumices were studied for whole rock chemistry and mineralogy by various workers (Iyer and Sudhakar, 1993; Martín-Barajas and Lallier-Verges, 1993; Mudholkar and Fujii, 1995; Iyer, 1996; Pattan et al., 2008). Detailed investigations of the morphology and petrography of tens of pumices were reported by Kalangutkar et al. (2011).The different types of pumices and their sources were later attested by a comprehensive investigation of the CIOB pumices by considering their chemical compositions (Kalangutkar, 2012).

The Indian Ocean pumices in general and particularly those in the CIOB have been suggested to be largely derived from the eruption of Krakatau (in 1883) and drifted to the basin (Frick and Kent, 1984; Iyer and Karisiddaiah, 1988; Mudholkar and Fujii, 1995; Mukherjee and Iyer, 1999; Pattan et al., 2008). Nevertheless, Iyer and Sudhakar (1993) had postulated a possible *in situ* submarine silicic volcanism to account for the derivation of the pumices.

Based on a study of the ferromanganese (FeMn) oxides that occur as coating over the CIOB pumices it was suggested that the pumices are between late Miocene and early Pleistocene and perhaps derived from the Indonesian Volcanic Arc (IVA) (Pattan et al., 2013, 2016). But by using empirical formulae based on Fe/Mn ratio it was opined that the ages of the oxides are between 7 Ma and 0.04 Ma which correspond to late Miocene to late Pleistocene periods (Kalangutkar et al., 2015). Furthermore, some of the pumices that form substrate for the FeMn oxides are older than late Miocene (Kalangutkar et al., 2015). Therefore, it is apparent that despite the availability of evidence for and against an *in situ* or IVA or Krakatau source, yet there is no single or more accepted source/s for the CIOB pumices.

It can be noted from the above information that there is a controversy concerning the derivation of the pumices and their occurrence in large numbers in the CIOB. Our objective is to document and classify a rich array of pumices in the CIOB. Based on mineralogical and petrographical variations we attribute the pumices to various volcanic sources that are within and around the CIOB. To our knowledge this is the first time that such parametres have been used to identify the possible sources of pumices to the basin.

2 Regional setting

The pumice samples for this study were recovered 9°–16°S, 72°–80°E in the CIOB and from an average water depth of 5 000 m (Fig. 1, Table 1). The FeMn nodules, encrustations and crusts were collected using free-fall grabs, Petterson grabs and dredges. Along with these materials, pumices that were invariably present

*Corresponding author, E-mail: niyati@unigoa.ac.in

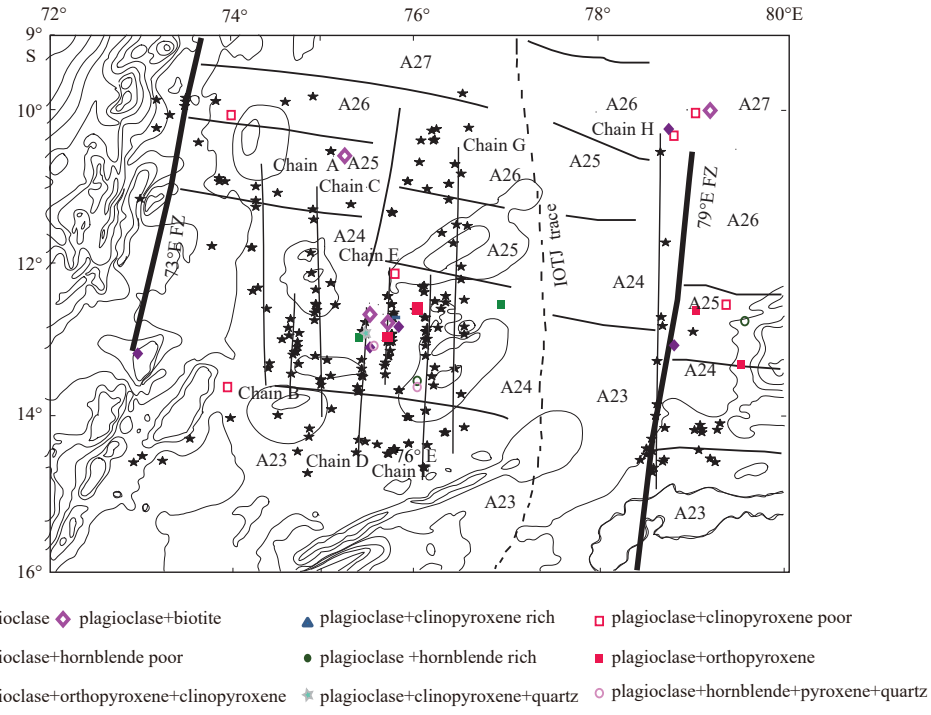

Fig. 1. Station location map for the studied Central Indian Ocean Basin pumices. A to H seamount chains along propagative fracture zones are shown. IOTJ: Indian Ocean Triple Junction; FZ: fracture zone. Contour intervals are in 100 m. Base map after Das et al. (2007). Mineral groups are as shown in Table 2. A23, A24, etc. are magnetic anomalies.

Table 1. Station location, water depth and morphology of pumices used in this study

No.	Station	a/cm	b/cm	c/cm	Shape	Latitude	Longitude	Water depth/m
1	F1/42 A	–	–	–	–	10.02°S	74.01°E	NA
2	AAS 26–5	7	5.5	3	oblate	12.52°S	75.69°E	NA
3	AAS 26–16	5	3	2.5	prolate	12.70°S	75.76°E	5 410
4	AAS 22–13	4	3.5	3	equant	12.08°S	75.80°E	5 220
5	F1/48D	–	–	–	–	13.08°S	73.01°E	5 114
6	F1/47D	–	–	–	–	13.50°S	73.99°E	5 088
7	SK 23/277D	–	–	–	–	11.00°S	78.74°E	5 110
8	SS13/696	3.2	2.8	2.1	equant	12.75°S	79.50°E	5 070
9	SS13/696	3.2	1.5	1	equant	12.75°S	79.50°E	5 070
10	AAS 27/12a	–	–	–	–	12.75°S	75.82°E	5 260
11	AAS 27/12b	–	–	–	–	12.75°S	75.82°E	5 260
12	SS6/372	–	–	–	–	11.00°S	78.00°E	NA
13	SS13/704C	7.5	5.3	2	oblate	12.45°S	79.30°E	5 250
14	AAS 26–9	15	11	3	oblate	12.50°S	75.67°E	5 260
15	AAS 3/B15/65a	6.8	6	4.8	equant	12.60°S	75.5°E	5 320
16	SK 23/255 B	7	5	4	equant	9.99°S	78.97°E	5 260
17	AAS 26–33	13	9	9	equant	12.93°S	75.44°E	5 220
18	AAS 26–7	10	7	5	equant	12.54°S	75.67°E	5 180
19	AAS 26–46 B	9	6	4	equant	10.53°S	78.74°E	5 297
20	AAS 3/B15/57	13	7.7	5.5	prolate	10.54°S	75.21°E	5 281
21	SS 23/255 CD	7	5	4	equant	9.98°S	78.97°E	5 235
22	AAS 26–44	4	2	1	bladed	12.96°S	75.49°E	5 280
23	AAS 26–19	9.5	6	5	equant	12.74°S	75.75°E	5 350
24	SS7/435C	4.4	3.5	2.5	equant	10.23°S	78.77°E	5 400
25	AAS 26–14	9	5	4	prolate	12.52°S	75.52°E	5 230
26	SS13/683	7	5	5	equant	13.51°S	76.00°E	5 250
27	AAS 27/12c	–	–	–	–	12.75°S	75.82°E	5 260
28	AAS 26–43	18	10.5	4	bladed	12.98°S	75.51°E	5 265
29	AAS 26–27	10.5	5	3	bladed	12.71°S	75.72°E	5 360

to be continued

Continued from Table 1

No.	Station	a/cm	b/cm	c/cm	Shape	Latitude	Longitude	Water depth/m
30	AAS 26–43	11	10	6	oblate	12.97°S	75.51°E	5 265
31	AAS 26–31	10	5	1	bladed	12.89°S	75.39°E	5 210
32	AAS 26–30	10	6	3	bladed	12.88°S	75.39°E	NA
33	AAS3/B15/69	7.1	5.2	3	oblate	12.73°S	75.70°E	5 305
34	SS10/650C	5.6	3.1	1	bladed	12.46°S	76.89°E	5 350
35	AAS 22–16	11.5	11	6.2	oblate	12.49°S	76.02°E	5 280
36	SS13/691C	8.5	7	5	equant	13.51°S	76.00°E	5 250
37	SS13/691C	6.5	4	2.8	prolate	13.51°S	76.00°E	5 250
38	AAS 26–36	5	3	2	prolate	12.97°S	75.47°E	5 270
39	AAS 26–19	9.5	6	5	prolate	12.74°S	75.75°E	5 350
40	SS13/683 A	4	2	1	bladed	13.51°S	76.00°E	5 250
41	SS1/21B	4.4	2.7	2.4	equant	11.99°S	81.03°E	5 250
42	SS7/435F	4.4	3	2.7	equant	10.22°S	78.76°E	5 400
43	SS7/469 D	5.9	2.6	2	prolate	13.24°S	79.50°E	5 000
44	SS2/104C	3	2.4	1.6	equant	12.00°S	74.99°E	5 180
45	SS7/464E	4.8	2.9	1.4	bladed	12.97°S	78.75°E	5 100
46	AAS3/B15/67	4.2	3.1	1	prolate	12.73°S	75.69°E	5 299
47	AAS3/B15/65b	5.6	4.2	3.2	equant	12.62°S	75.57°E	5 320
48	AAS3/B15/59	8	5.3	4.5	prolate	13.49°S	76.99°E	5 356
49	F1/41B	–	–	–	–	13.49°S	76.99°E	5 356
50	SS12/676V	6.2	4.4	5	equant	12.53°S	79.01°E	5 270
51	SS13/704C	7.5	5.3	2	oblate	12.45°S	79.31°E	5 250
52	SS13/691A	5.5	5.1	4.1	equant	12.17°S	79.20°E	5 440
53	AAS3/B15/60	9.7	7.8	3.1	oblate	10.59°S	75.12°E	5 250
54	AAS3/B15/62	5.1	3.2	2.9	prolate	12.867°S	75.69°E	5 329

Note: a: length; b: width; c: height; NA: not available; – represents no data.

were collected and preserved. The study area includes a number of fracture zones (FZ) such as the 73°E (Vishnu FZ), 76°30′E (Triple Junction Trace- TJT) and 79°E (Indrani FZ) (Fig. 1). In addition, there are eight chains of seamounts of different morphology are located along N–S trending propagative fractures (Das et al., 2007) and isolated seamounts some of which have cratered tops (Kodagali, 1998). The petrology of the seamounts and seafloor indicated their contemporaneous formation since 60 Ma (Iyer et al., 2018; Mukhopadhyay et al., 2018).

3 Material and methods

Eighty pumice samples of different sizes and textures were ultra-sonically cleaned; oven dried and were observed under a binocular microscope (Kalangutkar et al., 2011). The shape and of the studied pumices were also determined (Table 1). Fifty four thin sections were prepared and examined for mineralogical and textural variations and on each thin section 500 counts of the minerals were made to determine the modal percentage. The grain size and percentage of each phenocryst (plagioclase, ortho-pyroxene, clino-pyroxene, hornblende and oxide) and total phenocrysts were noted. The vesicularity, glass percentage and the presence FeMn oxides in vesicles (if present) were also noted.

The surface features of the pumices were examined with an SEM-EDS at the Council of Scientific and Industrial Research-National Institute of Oceanography (CSIR-NIO), Goa. The system used was an JSM 5800 LV, JEOL fitted with an INCA Energy Dispersive Spectrometer (EDS). For Scanning Electron Microscopy (SEM) and EDS studies small pieces were chipped off from the pumice specimens and were placed on a carbon stub affixed with carbon tape and coated with carbon to help improve the sample conductivity during the analysis.

Based on petrographical features, grain size and freshness of the minerals, twenty polished thin sections were made for mineral analysis. The phenocrysts to be probed were identified and marked on the sections and analyzed using an JEOL SEM-EDX 840A probe at the Queensland University of Technology, Australia. Backscatter electron (BSE) images were obtained of each polished section to understand the compositional variation within the mineral grains. The data were processed after applying the ZAF correction.

To determine the mineralogy, twenty pumice samples were powdered in a Retsch PM 400-ball mill. X-ray diffraction (XRD) studies were made by using a Rigaku Ultima IV machine with Cu Kα as target. The analytical conditions were as follows: Scanning range between 8° 2θ and 45° 2θ; scan speed: 0.02° 2θ/s (or 1.2° 2θ/min) and the chart speed was 10 mm/2θ. By referring to the JCDPS cards, the minerals were identified by determining the "d" values of the intensity peaks produced by the phases present in the sample.

4 Results

4.1 *Physical descriptions*

An initial examination of 676 specimens (from which the presently studied 80 samples were selected) revealed two types of pumices: uncoated (75%) and coated with FeMn oxides (25%). The colour of the uncoated pumices ranges from white to light grey, and size varies from 0.25 cm to 12 cm in diameter. Most of the pumice clasts are well rounded to sub-rounded in shape. The shapes of the CIOB pumices are inconsistent with 32% being oblate, 31% equant, 21% prolate and 21% bladed (Kalangutkar et al., 2011) (Table 1). Vesicles in the pumices are both circular and elongated with diameters varying between 5 μm and 15 μm. A few well-developed crystals are present within the vesicles

(Kalangutkar et al., 2011). We did not find any direct correspondence between shape and size amongst the studied pumices.

4.2 *X-ray diffraction (XRD)*

The XRD profiles of the CIOB pumice indicated them to be highly silicic and glassy as evident from the hump between 20° and 30° (Poulsen et al., 1995; Kalangutkar et al., 2011) (Fig. 2). The major minerals are quartz and plagioclase (labradorite) while the less commonly occurring minerals are augite, hornblende, quartz, fayalite and hypersthenes (Fig. 2).

4.3 *Petrography and mineralogy*

Binocular microscopy of the pumices shows fibrous and oval to spherical vesicles and glassy webs. A few of the vesicles contain drusy crystals of quartz, phillipsite crystals, biota and FeMn micronodules (Iyer and Karisiddaiah, 1988; Kalangutkar et al., 2011). Examination of thin sections reveals phenocrysts of plagioclase, biotite, clinopyroxenes, hornblende, quartz and opaque minerals in a glassy and vesicular groundmass (Fig. 3). The vesicle shapes (spherical, oval, elongated) and sizes (20–400 μm) show intra- and inter-clast variations.

Based on the mineral assemblages and modal percentages, the 54 thin sections were classified into eight groups and in all these groups glass is omni-present (Table 2). The eight groups are as follows.

Group 1: (plagioclase) (17%)
Group 2: (plagioclase+clinopyroxenes) (19%)
Group 3: (plagioclase+orthopyroxenes) (19%)
Group 4: (plagioclase+biotite) (19%)
Group 5: (plagioclase+hornblende) (14%)
Group 6: (plagioclase+clinopyroxenes+orthopyroxenes) (6%)
Group 7: (plagioclase+hornblende+pyroxene+quartz) (3%)
Group 8: (plagioclase+clinopyroxenes+quartz) (3%)

It should be noted that since sizes of the pumice are less than 12 cm, the different mineral assemblages may occur in the different fragments from the same source. Hence, we wish to show that based on the abundance of ferromagnesian minerals at least four major groups can be identified. These are as follows:

Group 2 (plagioclase+clinopyroxenes); Group 3 (plagioclase+orthopyroxenes); Group 4 (plagioclase+biotite) and Group 5 (plagioclase+hornblende). Within these groups, sub-groups (Table 2) were made considering the abundance of the phenocrysts. Group 2 has two sub-groups (plagioclase+clinopyroxenes rich) and (plagioclase+clinopyroxenes poor). Also, Group 5 has two subgroups (hornblende rich+plagioclase poor) and (hornblende poor+ plagioclase rich). The major groups along with the subgroups showing different mineral assemblages were plotted on a bathymetry map to examine if there was any tendency of the groups to occur at a particular site (Fig. 1). Incidentally, no preferential affinity of the pumices with any of the seafloor features was noted. This observation rules out the possibility of a particular volcanic site to have produced pumices with unique and of a single mineral assemblage.

4.4 *Mineral and glass chemistry*

Textural and chemical zoning patterns of crystals have been used as guides in understanding magmatic processes. This is because the mineral phases have a tendency to record the processes occurring in the magmatic system during their growth (Allègre et al., 1981; Iyer and Banerjee 1998; Ginibre et al., 2007). The diagnostic signatures of such processes manifest in the form of compositional zones and twin crystals and, therefore, these can be used as tracers of the magmatic history. Microscopy studies show unzoned (Figs 3b, d) and compositional zoned plagioclase (Fig. 3e) while BSE images show plagioclase as phenocrysts and inclusions in some of the pyroxene and biotite grains (Fig. 4).

The mineral compositions of plagioclase (zoned and unzoned), pyroxene, hornblende, biotite, magnetite and glass were determined using an EDS. The mineralogical data of the CIOB pumice samples are compared with those of Krakatau, IVA and Andaman. This is because these areas, that border the CIOB, are the postulated sources for the pumices in the CIOB (Iyer and Karisiddaiah 1988; Mudholkar and Fujii, 1995; Frick and Kent, 1984; Mukherjee and Iyer, 1999; Pattan et al., 2008) and for the silicic glass shards that occur in the CIOB sediments (Mascarenhas et al., 2006).

Plagioclase: Plagioclase was observed to be the most dominant phenocryst phase and range from 1% to ~10% (avg 4.7%). The plagioclase crystals range in size from 0.1 mm to 1.6 mm (minor axis) and 0.2 mm to 2.8 mm (major axis). Plagioclase phenocrysts and lath shaped microlites show lamellar twinning. A few phenocrysts are fresh, euhedral, have well-defined oscillatory

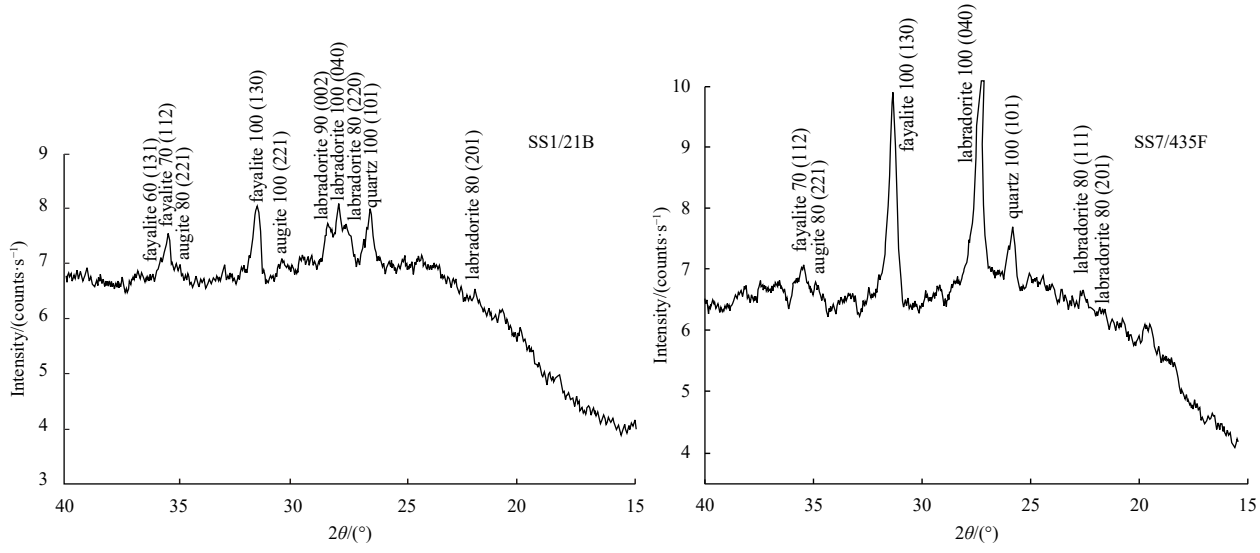

Fig. 2. X-ray diffraction of pumice showing the presence of different mineral phases: fayalite, augite, labradorite, and quartz.

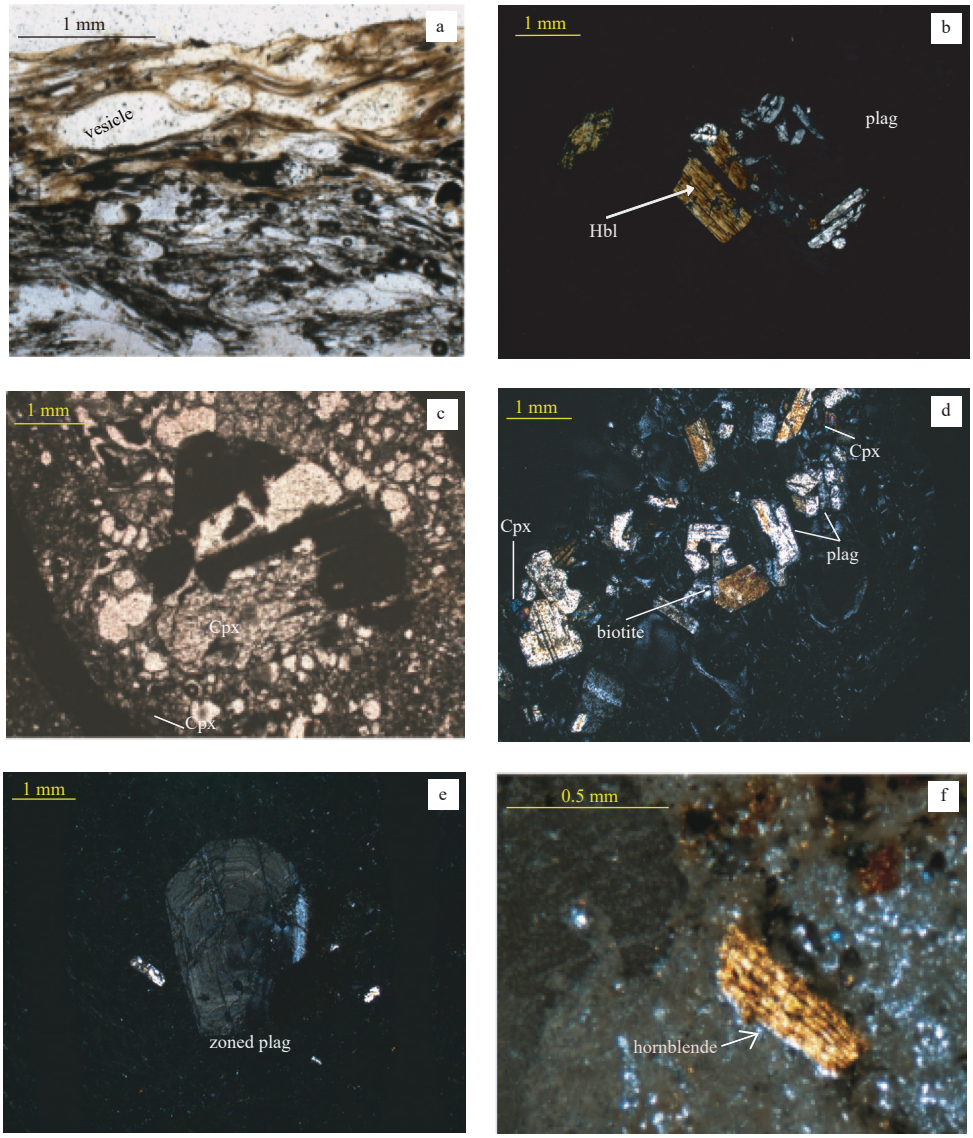

Fig. 3. Photomicrographs of pumices vesicles in glass (a), plagioclase and hornblende (b), biotite (c), glomeroporphyritic texture, plagioclase and clinopyroxenes (d), zoned plagioclase (e), hornblende (f).

Table 2. The sub-groups of pumice based on mineralogy within the major eight groups

Group 1	Group 2		Group 3	Group 4	Group 5		Group 6	Group 7	Group 8
Plag	Plag +Cpx		Plag+Opx	Plag+biotite	Plag+Hbl		Plag+Opx+ Cpx	Plag+Hbl+ Pyx+Qtz	Plag+Cpx+ Qtz
–	Cpx rich	Cpx poor	–	–	Hbl rich+Plag poor	Plag rich+ Hbl poor	–	–	–
AAS 26–44	AAS 26–19	SK 23/255B	SS10/650C	AAS 26–36	AAS 26–5 oblate	SS6/372	AAS 26–30	SS13/691C	SS1/21B
AAS 26–19	AAS 27/12	F1/47D	AAS 22–16	AAS 3/B15/57	AAS3/B15/67 prolate	SS13/683	SS10/650C	–	–
AAS 27/12	–	SS13/704C	AAS 26–31	SK 23/255 CD	–	SS13/696	–	–	–
F1/48D	–	SS7/435C	–	AAS 26–43	–	–	–	–	–
SS7/464E	–	F1/42A	AAS 26–43	AAS3/B15/59	–	–	–	–	–
SS7/435C	–	–	SS7/469D	AAS3 B15/65	–	–	–	–	–
–	–	–	SS13/704C	AAS 27/12	–	–	–	–	–
–	–	–	SS12/676V	–	–	–	–	–	–

Note: Plag: plagioclase; Cpx: clinopyroxene; Opx: orthopyroxene; Hbl: hornblende; Qtz: quartz; – represents no data.

zones (Fig. 3e) and do not have inclusions. There are two populations of plagioclase phenocrysts: twinned (and "fritted") and unzoned ones.

The average composition of plagioclase is SiO_2~57 wt%, Al_2O_3~27 wt%, CaO~8 wt%, and Na_2O~4 wt% (Table 3). The anorthite (An) content indicates the presence of labradoritic, bytownitic to anorthitic plagioclase composition (Fig. 5). It is observed that most of the phenocrysts have calcic cores (An_{54}–An_{88})

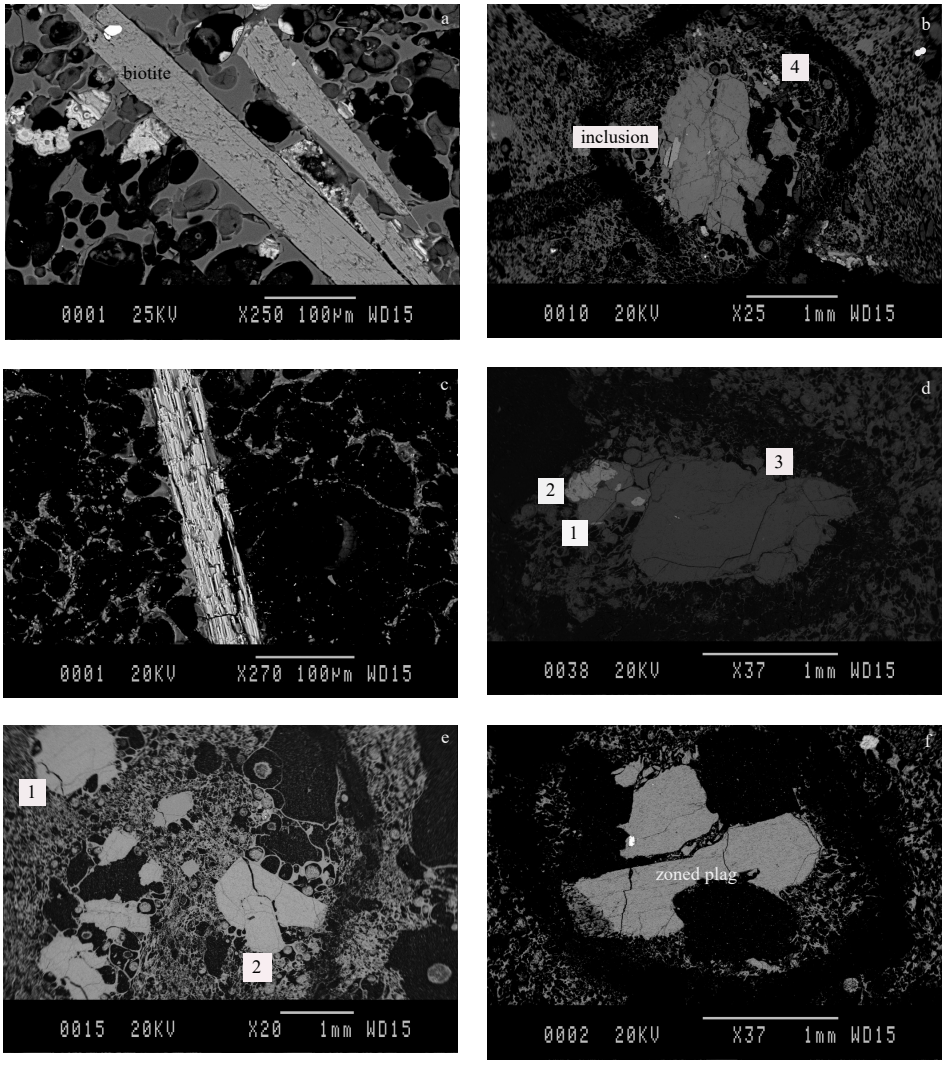

Fig. 4. Back scatter electron micrographs. a. Biotite crystals with oxide inclusion; b. plagioclase crystal with biotite inclusion; c. hornblende crystal; d. 3: plagioclase, 2: pyroxene, 1: iron oxide; e. 1: zoned plagioclase, 2: non-zoned plagioclase; f. zoned plagioclase.

and sodic rims (An_{44}–An_{87}) (Table 3).

We compared the plagioclase compositions of the CIOB pumices with those of Toba (Chesner, 1998) and Krakatau (Camus et al., 1987) (Fig. 5, Table 3). It is evident that the CIOB pumices do not belong to Younger Toba Tuff (YTT), Middle Toba Tuff (MTT) and Older Toba Tuff (OTT), but can be correlated with Haranggoal Dacite Tuff (HDT) and Krakatau 1883 eruption.

Andesite (age 1.8 Ma) from the Barren Island, Andaman shows the groundmass plagioclase to have An_{35}–An_{85} with phenocryst up to An_{91} (Ray et al., 2013) and these are compositionally similar to those of the CIOB pumices. The plagioclase phenocrysts from the Narcondam Island vary in composition from An_{44} to An_{81} while the groundmass plagioclases have An_{47}–An_{80} (Ray et al., 2011). The Andaman andesites host labradoritic, bytownitic and andesinic plagioclases while our pumices are devoid of andesinic but have anorthitic plagioclases.

Pyroxene: Glomeroporphyritic aggregates of plagioclase and clino- and/or ortho-pyroxenes were observed in most of the pumice samples (Fig. 3d). The modal analysis indicates clinopyroxenes to be marginally more (0.2% to 1.8%, avg 0.8%) than ortho-pyroxenes (0.2% to 1.2%, avg 0.55%). Mudholkar and Fujii (1995) had reported an abundance of clinopyroxenes over orthopyroxenes in the CIOB pumices. Pattan et al. (2013) reported the presence of orthopyroxenes in pumices that were either fully or partly coated with FeMn oxides but clinopyroxenes were absent. Probably this may be due to the fact that coated and uncoated pumices are not from the same source and are of different ages (Kalangutkar et al., 2015).

The clinopyroxene crystals in our samples range in size from 0.1 mm to 0.2 mm (minor axis) and 0.2 mm to 0.6 mm (major axis) while orthopyroxene crystals are 0.1 mm (minor axis) and 0.15 mm to 0.3 mm (major axis). A few of the pyroxene crystals has inclusions of iron-oxides while clinopyroxenes occur as inclusions in orthopyroxenes. We identified high Ca-rich clinopyroxene i.e., augite and diopside and also Ca-poor pigeonite and orthopyroxene (Table 4). Pigeonite has not been reported from the CIOB pumices and their present compositions do not correspond with the Andaman dacite-andesites reported by Pal et al. (2007). Several of the clino- and ortho-pyroxenes from the CIOB pumices are similar to the HDT and Krakatau pyroxenes (Fig. 6). The average composition of the CIOB pyroxenes is SiO_2~53 wt%, Al_2O_3~4 wt%, FeO~15 wt%, MgO~17 wt%, MnO~1.1 wt%, CaO~7 wt%, and Na_2O~0.3 wt%.

Hornblende: Hornblende grains are uncommon in the CIOB pumices and are reported for the first time (Table 5). Hornblende crystals have dimensions of 0.1 mm to 0.2 mm (minor ax-

Table 3. Microprobe analysis of core and rim of plagioclase grains in the Central Indian Ocean Basin pumices

Analysis of core of plagioclase grains														
Phenocrysts	Sample	SiO_2	TiO_2	Al_2O_3	FeO	MnO	BaO	CaO	Na_2O	K_2O	Total	An	Ab	Or
n=6	A42	56.17	bd	29.18	0.42	0.09	0.20	10.03	1.80	0.28	98.04	83.73	13.74	2.54
n=9	A39	57.75	0.11	27.80	0.42	0.11	0.07	8.70	2.15	0.13	97.39	78.98	19.82	1.20
n=3	S2	58.25	bd	26.60	0.20	0.38	bd	9.81	5.51	0.15	100.66	63.42	35.61	0.97
n=4	S1	54.36	0.07	26.03	0.47	0.04	0.04	9.43	5.23	0.18	97.13	63.75	35.33	0.92
n=2	A13	58.31	0.12	24.89	0.47	bd	0.02	7.82	6.18	0.34	98.67	54.46	43.21	2.34
n=1	S15	54.98	bd	25.82	0.47	0.11	0.03	9.69	5.21	0.16	97.27	64.34	34.59	1.06
n=4	A33	53.43	0.08	30.12	0.22	0.02	0.06	11.54	3.84	0.10	100.24	74.49	20.07	1.00
n=5	S7	61.24	bd	25.85	0.22	0.04	0.07	6.11	4.29	0.12	97.97	58.06	40.78	1.16
n=1	A15	57.05	bd	32.56	0.45	bd	0.17	9.85	1.25	0.05	101.80	88.34	11.21	0.45
Analysis of rim of plagioclase grains														
Phenocrysts	Sample	SiO_2	TiO_2	Al_2O_3	FeO	MnO	BaO	CaO	Na_2O	K_2O	Total	An	Ab	Or
n=5	A42	56.43	bd	29.11	0.43	0.07	0.24	10.13	1.44	0.26	97.92	87.34	10.37	2.28
n=8	A39	57.88	0.07	27.70	0.47	0.18	0.08	8.47	2.43	0.12	97.30	76.79	22.12	1.09
n=4	S2	61.71	0.13	22.93	0.19	0.29	bd	5.99	6.98	0.45	98.33	44.98	52.51	2.52
n=3	S1	55.32	0.06	25.56	0.41	0.11	0.13	9.19	5.40	0.16	97.03	62.33	36.61	1.06
n=3	A15	57.20	bd	32.49	0.44	0.08	0.12	9.72	1.31	0.08	101.69	87.46	11.85	0.69
n=1	S9	57.83	0.02	25.56	0.21	bd	0.11	7.74	6.32	0.24	98.80	54.13	44.20	1.68
n=2	A13	57.73	0.06	25.30	0.46	bd	0.05	8.36	5.94	0.21	98.47	57.60	40.95	1.46
n=1	S15	57.62	bd	25.51	0.41	0.03	bd	8.58	5.71	0.06	98.39	59.79	39.79	0.42
n=2	A33	57.85	0.08	27.29	0.17	0.05	bd	8.31	5.97	0.13	100.63	57.71	41.43	0.87
n=1	S9	57.83	0.02	25.56	0.21	bd	0.11	7.74	6.32	0.24	98.80	54.13	44.20	1.68
n=2	A30	57.28	bd	28.03	0.47	bd	0.18	8.87	2.01	0.27	97.49	79.55	18.03	2.42
n=2	S7	61.85	bd	25.58	0.19	0.03	0.03	5.75	4.65	0.17	98.29	54.31	44.10	1.61
n=1	A31	58.36	0.03	28.00	0.47	bd	0.03	8.55	2.83	0.26	98.52	73.45	24.31	2.23

Note: bd: below detection.

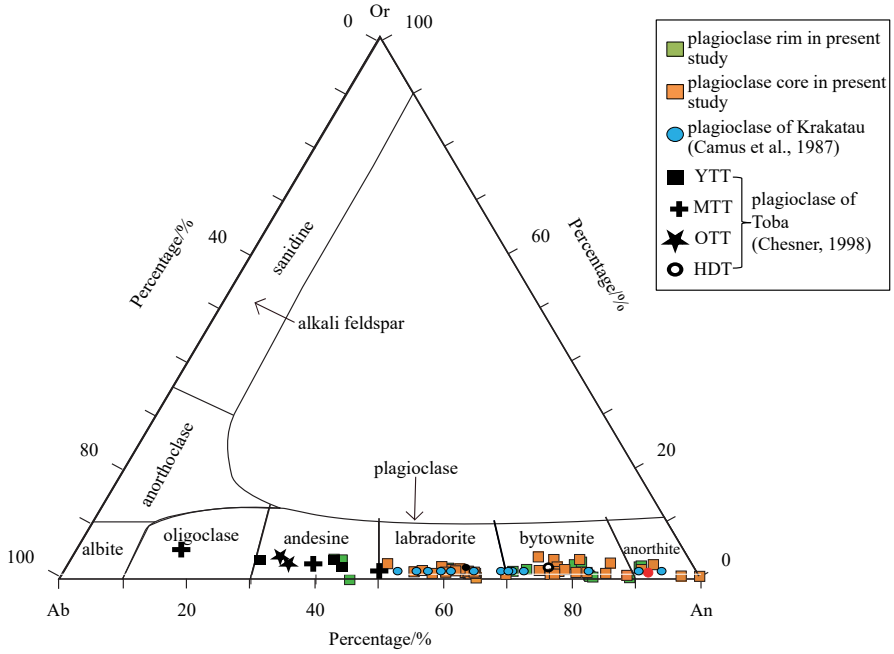

Fig. 5. The plot displays the rim and core compositions for the plagioclases of the Central Indian Ocean Basin, plagioclases of Krakatau pumices (Camus et al., 1987) and plagioclase composition of Toba pumices (Chesner, 1998). YTT: Younger Toba Tuff; MTT: Middle Toba Tuff; OTT: Older Toba Tuff; HDT: Haranggoal Dacite Tuff. Or: orthoclase.

is) and 0.2 mm to 0.6 mm (major axis) and occur as microlites and phenocrysts. Some of the phenocrysts are slightly altered. Hornblende forms 0.4% to 2% (avg 1.2%) and co-occur with plagioclases (Fig. 3b) and/or biotites (Fig. 3f). The composition of the CIOB hornblende is SiO_2~50 wt%, TiO_2~1.5 wt%, Al_2O_3~6.6 wt%, FeO~12 wt%, MgO~14 wt%, MnO~0.2 wt%, CaO~10.2 wt%, Na_2O~1.7 wt%, and K_2O~0.2 wt%. Hornblende has not been reported from either Krakatau or Toba eruptives; hence the source for hornblende-bearing pumices may be different, as would be discussed later (Table 5).

Biotite: Biotite grains are present in a few of the pumices (Fig. 3c) and depict typical pleochroism in shades of brown. The grains are euhedral and are present along with plagioclase and/or hornblende as phenocrysts or as individual grains. The size of the biotite grains ranges from 0.05 mm to 0.4 mm (minor axis) and 0.1 mm to 0.6 mm (major axis) and the modal percentage is 0.2% to 0.4% (avg 0.35%). Biotite grains were also observed as inclusions in plagioclase while those of oxides occur in most of the biotite grains. The biotites in the CIOB pumices have a very low FeO/MgO (0.77) and higher values of MnO (0.36 wt%) and TiO_2 (5 wt%) (Table 6).

Quartz: Free quartz was observed in a few thin sections with a modal percentage of 0.4%. No free quartz has been reported from earlier studies of the CIOB pumices.

Iron-titanium (Fe-Ti) oxides: The Fe-Ti oxides form aggregates with pyroxenes, hornblende, biotite and plagioclase and were also present as inclusions within other minerals or as individual grains (Fig. 4a) and has a modal percent of 0.2% to 1.8%

Table 4. Microprobe analysis of pyroxene grains in the Central Indian Ocean Basin pumices

Phenocrysts	Sample	SiO_2	TiO_2	Al_2O_3	FeO	MnO	MgO	CaO	Na_2O	K_2O	Cr_2O_3	Total	Wo	En	Fs
n=25	A42	54.01	0.23	0.83	18.64	1.27	24.27	1.82	0.04	0.03	0.06	101.10	4.06	54.25	41.69
n=17	A30	53.22	0.28	0.62	19.28	1.22	19.71	4.64	0.10	0.02	bd	99.03	10.71	45.14	44.15
n=10	A31	53.62	0.43	0.63	21.19	1.21	22.97	1.04	0.04	0.50	bd	100.98	2.30	50.82	46.88
n=4	S7	53.29	0.62	2.53	25.70	1.29	14.24	2.12	0.23	0.03	bd	99.69	5.04	33.85	61.11
n=16	A39	53.56	0.38	1.00	15.93	1.40	21.03	6.91	0.10	0.10	0.26	100.34	16.06	47.78	36.16
n=6	S11	52.52	0.22	0.48	21.71	1.36	21.76	1.20	0.06	0.01	bd	99.26	2.68	48.72	48.60
n=1	S2	55.43	0.08	bd	16.72	2.56	27.06	0.60	bd	bd	bd	102.44	1.35	60.97	37.68
n=1	A15	54.89	0.54	2.01	7.82	0.53	17.59	17.81	0.15	bd	0.27	101.60	41.21	40.69	18.10
n=1	S1	54.09	0.25	0.74	21.15	1.52	23.37	1.30	0.04	bd	bd	102.45	2.84	51.01	46.15
n=5	A25	55.03	0.56	2.59	23.87	1.26	14.27	1.92	0.30	bd	bd	99.79	4.79	35.63	59.58
n=1	A2	49.99	1.99	13.56	7.93	1.19	15.73	9.81	0.95	0.32	bd	101.47	29.31	47.00	23.69
n=2	A13	52.48	0.05	1.09	20.95	1.27	21.99	0.35	bd	1.50	bd	99.66	0.81	50.80	bd
n=2	S15	52.90	0.04	0.44	26.61	1.49	17.97	0.29	bd	1.62	bd	101.33	0.64	40.05	59.32

Note: Wo: wollastonite; En: enstatite; Fs: ferrosilite; bd: below detection.

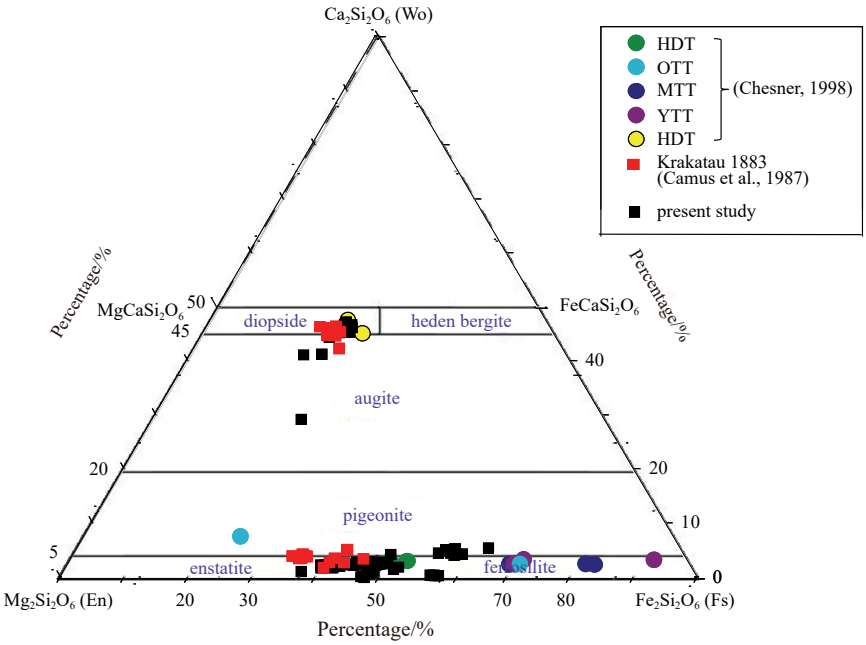

Fig. 6. Pyroxene classification diagram. Pyroxenes of the Central Indian Ocean Basin pumices plotted along with pyroxenes from Krakatau pumices (Camus et al., 1987) and pyroxenes from Toba eruptives (YTT, MTT, OTT) (Chesner, 1998). HDT: Haranggoal Dacite Tuff; OTT: Older Toba Tuff ; MTT: Middle Toba Tuff; YTT: Younger Toba Tuff; HDT: Haranggoal Dacite Tuff.

Table 5. Electron Dispersive Spectroscopy analysis of hornblende grains in Sample A33 (AAS26–43)

Phenocrysts	Sample	SiO_2	TiO_2	Al_2O_3	FeO	MnO	MgO	CaO	Na_2O	K_2O	Total
n=5	A33	50.52	1.4	6.636	12.602	0.265	14.65	10.285	1.72	0.266	96.27

Table 6. Microprobe analysis of biotites grains in Sample A25 (AAS 3/B15/57)

Phenocrysts	Sample	SiO_2	TiO_2	Al_2O_3	FeO	MnO	MgO	CaO	Na_2O	K_2O	Total
n=5	A33	50.52	1.4	6.636	12.602	0.265	14.65	10.285	1.72	0.266	96.27

(0.33) (Table 7). The Fe-Ti oxides with TiO_2 (6–47 wt%), FeO (48–87 wt%) and very low CaO (<1 wt%), fall in the ulvospinel zone while a few plots close to wustite and ilmenite fields (Fig. 7). Ulvospinel is being reported for the first time in the CIOB pumices while titano-magnetite (Oba et al., 1983) and ilmenite (Camus et al., 1987) are present in the Krakatau pumices.

Glass: The glassy groundmass is the most abundant phase in the CIOB pumices and has a modal percentage ranging from 33% to 54% (avg 43%). The glass either shows isolated, non-connected, oval, augen-shaped vesicles or has highly fibrous, well-connected vesicles and exhibits a swirled texture (Fig. 3a). In several samples, the glass is quite fresh and has SiO_2 from 52 wt% to 80 wt%, TiO_2 0.6 wt% to 1.0 wt%, FeO 0.8 wt% to 12.6 wt%, MgO 1 wt% to 3 wt% and K_2O 0.7 wt% to 4.3 wt% (Table 8).

The major oxides of the CIOB pumices are as follows, SiO_2 60 wt% to 75 wt%, TiO_2 0.14 wt% to 1.06 wt%, Al_2O_3 12 wt% to

Table 7. Microprobe analysis of iron-titanium oxides in the Central Indian Ocean Basin pumices

Phenocrysts	Sample	SiO_2	TiO_2	Al_2O_3	FeO	MnO	MgO	CaO	NiO	Cr_2O_3	Total
n=4	A42	0.02	12.20	2.90	81.54	0.85	2.33	0.07	0.02	0.11	99.98
n=3	A31	0.20	13.59	2.48	80.98	0.55	1.99	0.03	0.01	0.26	99.99
n=2	A39	0.12	17.29	2.39	77.01	0.75	2.02	0.04	0.01	0.21	99.72
n=2	S11	0.15	16.80	2.37	77.58	0.75	1.99	0.04	0.01	0.21	99.59
n=3	A32	0.15	14.83	2.38	79.44	0.95	1.99	0.04	0.03	0.18	99.30

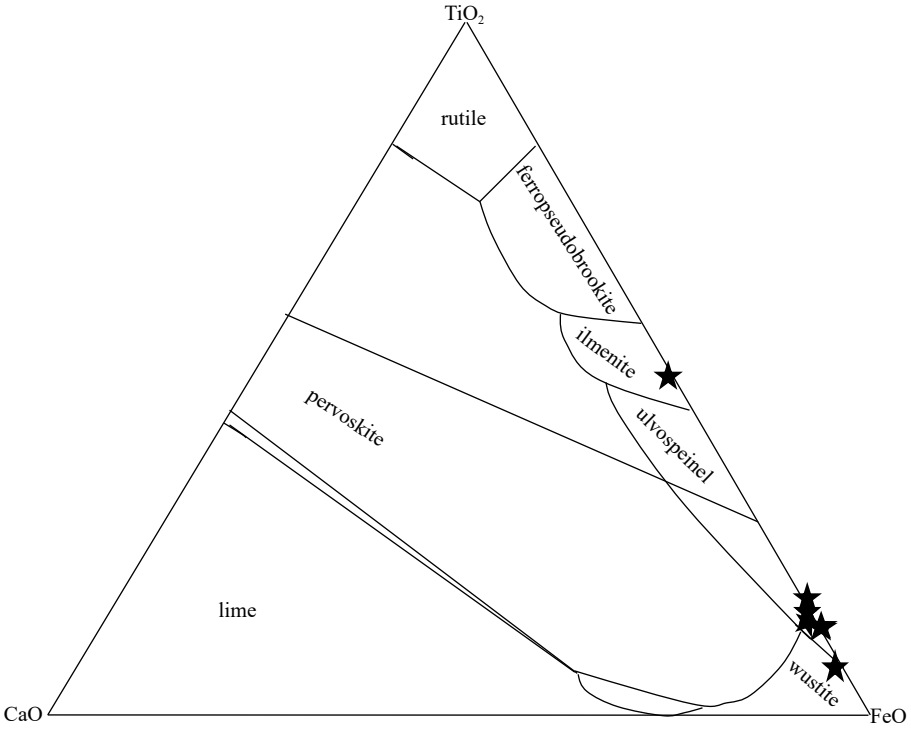

Fig. 7. Oxides-ilmenite-ulvospinel plot after Kimura and Muan (1971). The Fe-Ti oxides from the Central Indian Ocean Basin pumices plot within the ilmenite-ulvospinel field.

Table 8. Electron Dispersive Spectroscopy analysis of glassy matrix of the Central Indian Ocean Basin pumices

Sample	SiO_2	TiO_2	Al_2O_3	FeO	MnO	CaO	Na_2O	K_2O	MgO	Total
SS7-432D	52.07	1.04	17.57	12.63	0.45	8.90	3.54	0.69	3.12	100.01
SS7-437F	68.94	bd	11.16	8.24	0.52	2.53	4.13	1.40	3.07	99.99
SS7-474C	78.95	bd	12.05	0.84	bd	0.77	3.14	4.25	bd	100.00
SS7-474C	78.92	bd	12.00	0.81	bd	0.65	3.42	4.19	bd	99.99
SS2-66BG	63.26	1.30	13.35	8.82	bd	4.36	4.94	2.23	1.74	100.00
SS7-460C	69.26	0.77	11.60	4.58	bd	2.38	7.76	2.58	1.07	100.00
SS1-57A	68.09	0.61	12.25	3.90	bd	2.41	9.00	2.55	1.19	100.00
SS2-106C	59.55	1.40	15.14	9.12	0.47	5.16	4.27	2.77	2.12	100.00
SS2-106C	59.84	1.13	15.49	9.59	0.65	4.15	3.91	2.89	2.35	100.00
SS4-216 E	77.67	bd	12.17	1.65	bd	0.69	3.61	3.81	0.40	100.00
SS4-216 E	77.67	bd	12.17	1.65	bd	0.69	3.61	3.81	0.40	100.00
SS3 131 A,B	75.32	bd	12.00	3.02	bd	2.03	3.93	3.70	bd	100.00
AAS 26–19	79.80	bd	11.03	1.89	bd	0.53	2.91	3.84	bd	100.00

Note: bd: below detection.

17 wt%, FeO 1 wt% to 8 wt%, MnO 0.05 wt% to 3 wt%, MgO from 0.22 wt% to 2 wt%, CaO 0.8 wt% to 6 wt%, Na_2O 3 wt% to 5 wt%, K_2O 0.81 wt% to 5 wt% and P_2O_5 0.02 wt% to 0.4 wt% (Kalangutkar, 2012). We have initiated detailed geochemical studies of the various pumices that will help to confirm their sources in the CIOB. Similar studies have been reported for the Okinawa Trough by Shinjo and Kato (2000), Guo et al. (2018), Chen et al. (2020).

5 Discussion

We now discuss the results that were obtained through XRD analysis, microscopy observations, petrographical features and mineral compositions of the CIOB pumices. Further, a comparison of the characteristics of the CIOB pumices is made with those that erupted in the vicinity of the basin (Table 9). Finally, we provide evidence that either supports or rules out some of the postulated eruptive source/s to have contributed drift pumices to the CIOB.

XRD profiles revealed the presence of plagioclase, quartz, hornblende, augite and fayalite (Fig. 2) and these were confirmed through petrographic examinations. As stated earlier, based on the presence of ferromagnesian minerals, the CIOB pumices form eight groups and of these the dominant groups are: Group 2: plagioclase+clinopyroxenes, Group3: plagioclase+orthopyroxenes, Group 4: plagioclase+hornblende and Group 5:

Table 9. Comparison of the mineral assemblages of the Central Indian Ocean Basin (CIOB) pumices with those in the vicinity of the basin

Samples	Mineral assemblage	Reference
CIOB pumices	plagioclases 1.1% to 9.6% (4.7%) clinopyroxene 0.2% to 1.8% (0.8%) orthopyroxene 0.2% to 1.2% (0.55%) biotite 0.2% to 0.4% (0.35%) hornblende 0.4% to 2% (1.2%) quartz (0.4%) (±fayalite+oxides) vesicles 33% to 45.4% (38.2%) glass 32.8% to 53.86% (42.6%)	present work
Krakatau 1883 pumice	white band grey band plagioclase (12%) (7.5%) clinopyroxene (rare) (2%) orthopyroxene (rare) (0.5%) oxide (rare) (1%) hornblende, biotite, quartz (not present)	Camus et al. (1987)
Krakatau 1883 pumice	plagioclase (5.7%) clinopyroxene (0.4%) orthopyroxene (0.6%) oxide (1.1%) vesicles (92%)	Oba et al. (1983)
Anak 1927–1979 pumice	plagioclase (29%) olivine (2.5%) (sometimes jacketed by Opx)	Oba et al. (1983)
Anak 1981 pumice	clino- and ortho- pyroxene (3%) magnetite oxide (1%)	Oba et al. (1983)
	plagioclase (23%) clinopyroxene (3%) orthopyroxene (3.5%) magnetite and ilmenite oxide (2%)	
Andaman, Barren and Narcondam andesite and dacite rocks	calcic and sodic plagioclase, forsteritic olivine, clinopyroxene, orthopyroxene, hornblende, minor quartz and apatite, andesites and dacites (not pumice), hence modal proportions is not given	Ray et al. (2011)
Narcondam pumice	plagioclase, amphibole, pyroxene	Pal et al. (2007)
HDT Toba pumice	plagioclase, ortho- and clinopyroxene, magnetite, ilmenite	Chesner et al. (1998)
OTT Toba pumice	quartz, plagioclase, sanidine, biotite, amphibole, orthopyroxene, magnetite, ilmenite, allanite, zircon	
MTT Toba pumice	quartz, plagioclase, sanidine, biotite, amphibole, orthopyroxene, magnetite, ilmenite, allanite, fayalite, zircon	
YTT Toba pumice	quartz, plagioclase, sanidine, biotite, magnetite, ilmenite, allanite, fayalite, zircon, orthopyroxene	
Taupo, New Zealand pumice	plagioclase, orthopyroxene, quartz, hornblende, magnetite (as inclusions in orthopyroxene, plagioclase, hornblende or as microphenocrysts), ilmenite, acessory zircon and apatite (as inclusions in orthopyroxene, plagioclase and magnetite and as microphenocrysts)	Wilson et al. (2006)
South Sandwich pumice	plagioclase (andesine-labradorite), corroded feldspar (sanidine-anorthoclase), clinopyroxene (diopside or augite), orthopyroxene (hypersthene), red-brown hornblende, magnetite,vesicle (50%–60%)	Risso et al. (2002)
Tonga pumice	calcic plagioclase, augite, pigeonite, titanomagnetite	Bryan et al. (2004)
Kerguelen pumice lapilli layer in basaltic and silicic ash	fresh sanidine, Ab-rich plagioclase, hedenbergitic clinopyroxene, few quartz	Bitschene et al. (1992b)

plagioclase+biotite. Depending on the group, plagioclase, quartz, hornblende and augite occur as phenocrysts of variable sizes. The modal percentage in the studied samples show up to 12.4% phenocrysts, glass 33% to 54% and vesicles 29% to 54%.

The observed range of phenocryst chemistry and zoning of plagioclases are indicative of their formational conditions and variable magma compositions. Perhaps the source magma erupted under polybaric conditions and the pumices represent composite products of more than one petrogenetic stages and/or sources. The phenocrysts of plagioclase show fine concentric zoning along the rim and suggest changing pressure (*P*), temperature (*T*) and/or water conditions. This could be due to an increase in water pressure during ascent of magma (cf. Vance, 1965; Almeev and Ariskin, 1996) which led to the crystallisation of sodic plagioclase, perhaps due to an influx of Ca-rich magma or due to magma mixing. Since zoning in plagioclase is inversely related to ascent rate of magma (Fisk, 1984), the CIOB pumices with zoned plagioclases indicate a rapid cooling of the lava and insufficient time for the crystals to equilibrate with the host melt. We suggest that the lowering of pressure during magma ascent may have led to fracturing and resorption and recrystallisation of the plagioclase grains.

The plagioclases in the CIOB pumices are labradoritic, bytownitic and anorthitic in composition (Fig. 6) and most of the normal zoned phenocrysts (Samples S9, S7, S15, A33) show compositional differences and have calcic cores (An_{50}–An_{96}) (Table 3) and sodic rims (An_{41}–An_{88}) (Table 3). From the observations it can be said that these compositional changes could have been caused by rhythmic changes in the magma chemistry.

Some of the studied pumices show resorbed margin of quartz grains which again indicate fluctuating magma temperature and this is supported by the presence of zoned plagioclase that suggest variable magma composition or mixing of magmas (cf. Hibbard, 1981; Müller et al., 2005). Magma mixing could also result in rapid crystallisation and build-up of volatiles in the magmatic mush (Cox and Bell, 1972) which can trigger vesiculation and explosion (Clynne, 1999). This fact is reinforced by the occurrence of hydrous minerals like biotite and hornblende in the CIOB pumices and implies their formation in the presence of high contents of volatiles or interaction with water during crystallisation (cf. Beard et al., 2004).

5.1 *Comparisons with other pumices*

We now compare the mineral assemblages of the CIOB pumices with those of the submarine silicic volcanics surrounding the study area, so as to identify if any of the terrestrial volcanoes may have contributed pumices to the CIOB (Table 9).

Andaman-Narcondam: Pal et al. (2007) identified vesicular glass-rich pumices in the Andaman. These had resorbed plagioclase and sometimes clinopyroxenes and amphibole within a glassy mass that produced a sieve texture in the xenoliths. But no further data about the pumices are available for comparison.

"Fritted" plagioclase, similar to those observed by Ray et al. (2011) in the Andaman rocks, has also been observed in a few of our CIOB samples. Labradoritic, bytownitic and anorthitic composition of plagioclase in the pumices are akin to those from Narcondam volcanic that are a product of mixing of basic (andesitic) and acidic (rhyolitic) magmas (Pal et al., 2007; Ray et al., 2011). Silicic magma produces foam (Clynne, 1999) and the formation of such foam at Andaman-Narcondam perhaps resulted in the breaking of several pumice blocks due to instability and their subsequent drift to the CIOB; but this possibility needs further confirmation.

South Sandwich Island: The micro phenocrysts of plagioclase in the South Sandwich (Southern Atlantic Ocean). Pumices occur as individual phenocrysts or in an ophitic arrangement and form less than 5% while vesicles make up 50%–60%. The plagioclases (andesine-labradorite) are mostly euhedral in shape and are zoned. The associated minerals are corroded K-feldspar (sanidine-anorthoclase), clinopyroxene (diopside or augite), orthopyroxene (hypersthene), magnetite and red-brown hornblende (Risso et al., 2002). Though labradoritic plagioclase occurs in the CIOB pumices but alkali feldspars are absent. Hence, the South Sandwich Island as a source for the CIOB pumices seems to be doubtful.

Tonga volcano: The Tonga volcano pumices have calcic plagioclase, augite, pigeonite and titano-magnetite (Bryan et al., 2004). This mineral assemblage is similar to that observed in most of the examined CIOB pumices. Some of the pigeonite composition of our samples is akin to those from the 1964 pumice eruption of Tonga. Though the orthopyroxenes from the CIOB pumices show similarity to 1964 Tonga pumice but lie between the compositions of oldest (3.5–1.8 ka) and youngest (September 2001) eruptions of Tonga (Bryan et al., 2004).

Kerguelen Plateau: The Kerguelen Plateau is known to have erupted voluminous basaltic lavas (Bitschene et al., 1992a, b) but phases of silicic volcanism occurred in late Miocene and Pliocene with the major volcanic activity in the northern Kerguelen Plateau (Bitschene and Schmincke, 1990). These volcanics contain Na and Fe-rich pyroxenes, alkali feldspar, apatite and Ti-magnetite with subordinate biotite and zircon. Pumice has also been reported from Ocean Drilling Program (ODP) and Deep Sea Drilling Project (DSDP) Legs 119 and 120 and comprise Site 736 (Leg 119) from the Kerguelen Plateau. The younger pumices are of Quaternary age while the older ones are of Oligocene to Pliocene age (Kidd et al., 1992).

Frey et al. (2000) recovered a 20 m thick volcano-clastic succession containing six trachytic pumice-lithic breccias deposited by pyroclastic flows from the Central Kerguelen Plateau. Bitschene et al. (1992b) reported the occurrence of 90%–95% of blocky to well-rounded, silicic, highly vesicular pumice lapilli layer containing fresh sanidine, Ab-rich plagioclase, hedenbergitic clinopyroxene, quartz and biotite along with basaltic and silicic ash from the Kerguelene Plateau. Such mineral assemblages are absent in our pumices hence, Kerguelene is ruled out as a source for the CIOB pumices.

Krakatau (in 1883): It is observed that the eruption of Krakatau (in 1883) produced pumices with minerals and modal assemblages that are largely comparable to some of our samples though hornblende and biotite have not been reported from Krakatau. This suggests that the hornblende and biotite containing pumices of the CIOB may have a different source. We also rule out the younger eruptions from Krakatau, the Anak 1927–1979 and Anak 1981 as sources because these have higher modal percentage 29% and 23%, respectively (Oba et al., 1983) than our samples (3%–19%).

Toba: The Toba volcano in the IVA had four major eruptions: YTT, MTT, OTT and HDT and these have ages of 0.074 Ma, 0.50 Ma, 0.84 Ma and 1.20 Ma, respectively (Chesner, 1998). The pumices of these eruptions have quartz, plagioclase, sanidine, biotite, magnetite, ilmenite, allanite, fayalite, zircon and orthopyroxene (Chesner, 1998). Of these, allanite, zircon and sanidine are absent in the CIOB pumices. The HDT bears plagioclase, ortho- and clinopyroxenes, magnetite and ilmenite and this assemblage is comparable to that found in our pumices.

Taupo, New Zealand: The Taupo volcanics of New Zealand

shows plagioclase, orthopyroxene, quartz, hornblende, magnetite, ilmenite, zircon and apatite (Wilson et al., 2006). Although apatite is reported as an accessory mineral in ortho- and clino-pyroxenes in only two pumices (Mudholkar and Fujii, 1995) but none of the 54 specimens we examined have apatite. Hence, Taupo may not be the source for the CIOB pumices under investigation.

In the light of the above findings, it is clear that some of the external sources could be ruled out as contributors for the CIOB pumices. This leaves us with three probable sources: Krakatau volcano (Iyer and Karisiddaiah, 1988; Mudholkar and Fujii, 1995), the several eruptions of Toba (Chesner, 1998) and possibility of intraplate silicic volcanism (Iyer and Sudhakar, 1993; Iyer, 1996; Mukherjee and Iyer, 1999).

Based on the mineral chemistry of our investigations we confirm the Krakatau volcano as one of the sources for the CIOB pumices. This is also borne out by the fact that the August 26–27, 1883 eruption of Krakatau volcano (Indonesia) resulted in pumice blocks that drifted across the Indian Ocean and were even found along the beaches of the East coast of Africa (Frick and Kent, 1984). However, it was reported that in the absence of favourable surface current circulation patterns, Krakatoan volcanic products may not occur in any significant amount in the recent sediments east of 80°E (Svalnov, 1981).

Although the YTT as a source was suggested (Pattan et al., 2008, 2013), we negate this view because the YTT eruption largely produced huge amounts of silicic glass shards and hardly any pumices (Chesner and Rose, 1991). There are several studies concerning the extensive occurrence of glass shards in the CIOB sediments but there is no mention about the find of YTT pumices (Amonkar et al., 2020 and references therein). It appears that the HDT eruption may have contributed some of the pumices to the CIOB. There is no reported occurrence of biotite in pumice from Krakatau 1883 eruption (Camus et al., 1987; Oba et al., 1983). Similarly, hornblende has not been reported from Toba (Chesner, 1998) and Krakatau (Camus et al., 1987; Oba et al., 1983). Hence, biotite-and hornblende-bearing CIOB pumices may be from unknown terrestrial sources or from *in situ* eruption.

5.2 *The explosive eruptions in the deep sea*

Pumice clasts recovered from abyssal depths are considered to be exotic because of the constraints in their formation yet; there are several reports of pumices in the deep sea. For example, in the Atlantic Ocean pumice was reported over submarine volcanoes at depths of 1 500 m to 2 000 m (Neumann von Padang, 1967), near Tonga depths at >1 500 m (Fouquet et al., 1991) Okinawa Trough, South of Japan (Halbach et al., 1989) and trachytic pumice flows (with hydrothermal crusts) occur at intraplate volcanoes in the Society and Austral hotspot regions (water depth=3 500 m; Binard et al., 1992). Silicic volcanism at an off-axis geothermal field in the Mariana Trough resulted in rhyodacitic pumice between 2 600 m and 3 600 m water depth. A possible suggested source for the silicic magma was ascribed to melting of the sea floor sediments during volcanisms and the sediments include altered volcano clastic debris from the adjacent island arc and siliceous hemipelagic muds (Lonsdale and Hawkins, 1985).

Hédervari (1982) reported the presence of pumices at water depths >1 500 m in the Indian Ocean. He opined the pumices to have originated from an inferred submarine volcano near the central part of the Ninety East Ridge. Studies by Iyer and Sudhakar (1993, 1995) led to the postulation of a seemingly possible *in situ* submarine silicic volcanism as a source of pumice in the CIOB.

Explosive eruptions could be possible at water depths in excess of 3 000 m (Kalangutkar and Iyer, 2012), leading to the production of a wide range of pyroclastic deposits (Head and Wilson, 2003). Deposits of fragmented rhyolitic pumice and basaltic scoria that erupted subaqueously have been found in several places in the world ocean, at depths up to 2 000 m (Kato, 1987; Cashman and Fiske, 1991; Fiske et al., 1998). Studies by various researchers suggest potential submarine explosive eruption styles that include Plinian (sustained discharge of volatile-rich magma; Kokelaar and Busby, 1992; Kano, 2003), vulcanian (short-lived explosion resulting from failure of a solid plug in the vent), strombolian (bursting of large bubbles in low-viscosity magma), and fire fountaining (eruption of low viscosity magma in the form a spray; Mueller and White, 1992; Head and Wilson, 2003).

The paradigm of deep sea silicic volcanism has gained ground considering the recent studies of silicic volcanic glass shards of the CIOB. Detailed investigations revealed that although Toba glass shards of 74 ka are ubiquitous in the basin, however there are strombolian-type shards that seemingly have no age correlations with the Toba event. Based on $^{230}Th_{excess}$ values and radiolarian stratigraphy, Sukumaran et al. (1998) opined that the shards were deposited *in situ* as a consequence of suboceanic volcanic activities during periods of elevated glaciation. Considering the morphology, occurrence and age of the shards; localized, *in-situ* phreatomagmatic episodes have been proposed to account for the origin of the shards (Iyer et al., 1997; Mascarenhas-Pereira et al., 2006; Amonkar et al., 2020).

Collectively, the above discoveries strongly suggest that silicic volcanic products may have recently erupted at great depths from submarine volcanoes. Interestingly, large pumice clasts that have been frequently recovered from the CIOB may indicate that they had short flotation times and derived from intraplate volcanoes (Iyer and Sudhakar, 1993) because locally derived hot pumices have a tendency to sink faster and near to the volcanic source (cf. Whitham and Sparks, 1986).

5.3 *The in situ origin, transport and deposit mechanism*

The shapes of the CIOB pumices are variable: 32% oblate, 31% are equant, 21% prolate and 21% bladed (Kalangutkar et al., 2011). It is believed that the clasts with other than equant size may be derived from a source nearer to the site of deposition, which could be within or near the CIOB. The eight groups of pumice that were identified based on mineralogy have the following shapes.

Group 1: either equant/bladed/prolate
Group 2: equant/prolate and oblate
Group 3: equant followed by oblate, prolate/bladed
Group 4: either equant/prolate/bladed
Group 5: oblate and prolate
Group 6: bladed
Group 7: equant
Group 8: equant

The above mineral groups when correlated with the Zings classification (Kalangutkar et al., 2011), indicates that most of the groups have clasts which are either oblate, prolate or bladed while equant is dominant in a few groups, e.g., Groups 2 and 3 (Table 2). This suggests that equant pumice clasts perhaps travelled from a distant source and this is also supported by the mineral composition studies that are comparable with those of the pumices from HDT of Toba and Krakatau (Figs 5 and 6). The non-equant clasts that are oblate or prolate may have settled rapidly near the source of formation, since hot pumice tends to sink near the source of formation (Whitham and Sparks, 1986).

The drift of the pumices into the present site from the nearby possible volcanic sources can be explained by water circulation pattern as shown in Fig. 8.

Silicic shards of rhyolitic composition of *in situ* origin (phreatomagmatic eruption) along flanks of a seamount and in the vicinity of 76°30′E FZ, assumed to be formed due to possibility of reactivation of tectonic activity in the faulted area (Mascarenhas-Pereira et al., 2006) and also in other regions of the basin (Amonkar et al., 2020). The evidence perhaps indicates sporadic intraplate silicic volcanism near seamounts and FZ in the CIOB.

6 Conclusions

(1) Based on the mineral assemblages we have identified eight groups of pumices in the CIOB. All the pumices were not derived from Krakatau volcano and nor from YTT, MTT, and OTT eruptions of the IVA, as was suggested by earlier researchers.

(2) The pumices of Group 2 (plagioclase+clinopyroxenes) and Group 3 (plagioclase+orthopyroxenes) are comparable to those from HDT of Toba and Krakatau in terms of mineralogy and are equant clasts in size indicating distant source. Hence, it can be inferred that perhaps HDT and Krakatau pumices drifted and reached the CIOB.

(3) Pumices similar to Group 1 (plagioclase), Group 4 (plagioclase+biotite), Group 5 (plagioclase+hornblende) and Group 6 (plagioclase+orthopyroxe+clinopyroxene) have not been reported from Toba, Krakatau and from Andaman-Narcondam. These are mostly the non-equant clasts which may have settled rapidly near the source of formation. Therefore, the pumices of these groups are ascribed to plausible silicic eruptions in the CIOB.

(4) Group 7 (plagioclase+hornblende+pyroxene+quartz) and Group 8 (plagioclase +clinopyroxene+quartz) are from unknown source and require a more detail study.

(5) Pigeonite, fayalite and ulvospinelare noted for the first time in the CIOB pumices.

It is concluded that the mineralogy and mineral compositions together with morphology can be used to study the source of pumices in the CIOB. The study indicates that the pumices have been derived from multiple terrestrial sources and also from intraplate volcanism. The present findings would be validated (manuscript under preparation) by taking recourse to the geochemical characteristics of the CIOB pumices and their comparison with their suggested sources of derivation.

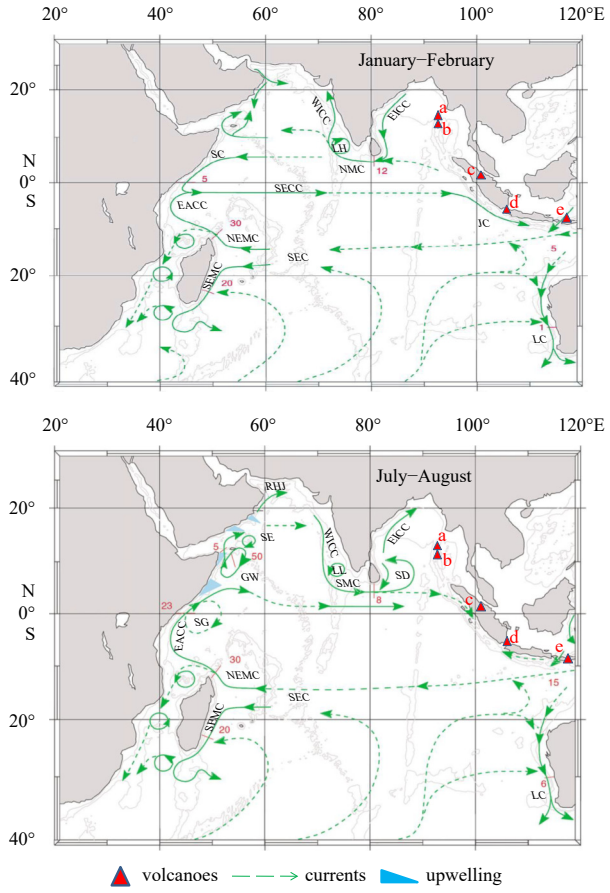

Fig. 8. A schematic representation of currents observed during the months January–February and July–August in the Indian Ocean. These currents may have helped to transport pumice clasts across the Indian Ocean from the nearby terrestrial volcanoes while the water-laden clasts may have sunk in the Central Indian Ocean Basin. The currents identified are: South Equatorial Current (SEC); South Equatorial Counter Current (SECC); Northeast and Southeast Madagascar Current (NEMC and SEMC); East Africa Coastal Current (EACC); Somali Current (SC), West India Coastal Current (WICC); Lakshadweep High (LH); East India Coastal Current (EICC); Northeast Monsoon Current (NMC); South Java Current (JC); and Leeuwin Current (LC). The Indo-Pacific Throughflow, which enters from the east, influences both the SEC and the LC. The base figure is modified from Schott and McCreary (2001). The volcanoes marked are Narcondum (a), Barren (b), Toba (c), Krakatau (d), and Tambora (e).

Acknowledgements

We thank the Director of Council of Scientific and Industrial Research-National Institute of Oceanography (CSIR-NIO), Dona Paula, Goa and Vice-Chancellor, Goa University for providing facilities and encouragements. Niyati G. Kalangutkar was supported by CSIR-SRF during her doctoral work at the CSIR-NIO. We acknowledge Vijay Khedekar and Areef Sardar, both from CSIR-NIO, for help during the SEM-EDS and EPMA analyses. Part of the research was supported under Endeavour Fellowship awarded to Niyati G. Kalangutkar by Government of Australia and the work was conducted at Queensland University of Technology Laboratory, Brisbane, Queensland. Niyati G. Kalangutkar is grateful to Scott Bryan who was the research supervisor during the Fellowship and extended instrument facilities. Thanks to the reviewers and EIC for comments which helped to review the manuscript.

References

Allègre C J, Provost A, Jaupart C. 1981. Oscillatory zoning: a pathological case of crystal growth. Nature, 294(5838): 223–228, doi: 10.1038/294223a0

Almeev R R, Ariskin A A. 1996. Mineral-melt equilibria in a hydrous basaltic system: computer modeling. Geochemistry International, 34(7): 563–573

Amonkar A, Iyer S D, Babu E V S S K, et al. 2020. Extending the limit of widespread dispersed Toba volcanic glass shards and identification of new *in-situ* volcanic events in the Central Indian Ocean Basin. Journal of Earth System Science, 129(1): 175, doi: 10.1007/s12040-020-01429-6

Beard J S, Ragland P C, Rushmer T. 2004. Hydration crystallization reactions between anhydrous minerals and hydrous melt to yield amphibole and biotite in igneous rocks: Description and Implications. The Journal of Geology, 112(5): 617–621, doi: 10.1086/422670

Binard N, Hékinian R, Cheminée J L, et al. 1992. Styles of eruptive activity on intraplate volcanoes in the Society and Austral hot

spot regions: bathymetry, petrology, and submersible observations. Journal of Geophysical Research: Solid Earth, 97(B10): 13999–14015, doi: 10.1029/92JB00692

Bitschene P R, Dehn J, Mehl K W, et al. 1992a. Explosive ocean island volcanism and seamount evolution in the Central Indian Ocean (Kerguelen Plateau). In: Duncan R A, Rea D K, Kidd R B, et al., eds. Synthesis of Results from Scientific Drilling in the Indian Ocean. Geophysical Monograph Series. Washington, DC: American Geophysical Union, 70: 105–113, doi: 10.1029/GM070p0105

Bitschene P R, Mehl K W, Schmincke H U. 1992b. Composition and origin of marine ash layers and epiclastic rocks from the Kerguelen Plateau, southern Indian Ocean (Legs 119 and 120). In: Wise S W Jr, Schlich R, et al., eds. Proceedings of the Ocean Drilling Program, Scientific Results. College Station, TX: Ocean Drilling Program, 120: 135–149

Bitschene P R, Schmincke H U. 1990. Fallout tephra layers: composition and significance. In: Heling D, Rothe P, Förstner U, et al., eds. Sediments and Environmental Geochemistry. Berlin, Heidelberg: Springer-Verlag, 48–82

Bryan S E, Cook A, Evans J P, et al. 2004. Pumice rafting and faunal dispersion during 2001–2002 in the Southwest Pacific: record of a dacitic submarine explosive eruption from Tonga. Earth and Planetary Science Letters, 227(1–2): 135–154

Camus G, Gourgaud A, Vincent P M. 1987. Petrologic evolution of Krakatau (Indonesia): Implications for a future activity. Journal of Volcanology and Geothermal Research, 33(4): 299–316, doi: 10.1016/0377-0273(87)90020-5

Cashman K V, Fiske R S. 1991. Fallout of pyroclastic debris from submarine volcanic eruptions. Science, 253(5017): 275–280, doi: 10.1126/science.253.5017.275

Chen Zuxing, Zeng Zhigang, Wang Xiaoyuan, et al. 2020. Element and Sr isotope zoning in plagioclase in the dacites from the southwestern Okinawa Trough: Insights into magma mixing processes and time scales. Lithos, 376–377: 105776, doi: 10.1016/j.lithos.2020.105776

Chesner C A. 1998. Petrogenesis of the Toba Tuffs, Sumatra, Indonesia. Journal of Petrology, 39(3): 397–438, doi: 10.1093/petroj/39.3.397

Chesner C A, Rose W I. 1991. Stratigraphy of the Toba Tuffs and the evolution of the Toba Caldera complex, Sumatra, Indonesia. Bulletin of Volcanology, 53(5): 343–356, doi: 10.1007/BF00280226

Clynne M A. 1999. A complex magma mixing origin for rocks erupted in 1915, Lassen Peak, California. Journal of Petrology, 40(1): 105–132, doi: 10.1093/petroj/40.1.105

Cox K G, Bell J D. 1972. A crystal fractionation model for the basaltic rocks of the New Georgia Group, British Solomon Islands. Contributions to Mineralogy and Petrology, 37(1): 1–13, doi: 10.1007/BF00377302

Das P, Iyer S D, Kodagali V N. 2007. Morphological characteristics and emplacement mechanism of the seamounts in the Central Indian Ocean Basin. Tectonophysics, 443(1–2): 1–18, doi: 10.1016/j.tecto.2007.08.002

Fisk M R. 1984. Depths and temperatures of mid-ocean-ridge magma chambers and the composition of their source magmas. Geological Society, London, Special Publications, 13(1): 17–23, doi: 10.1144/GSL.SP.1984.013.01.02

Fiske R S, Cashman K V, Shibata A, et al. 1998. Tephra dispersal from Myojinsho, Japan, during its shallow submarine eruption of 1952–1953. Bulletin of Volcanology, 59(4): 262–275, doi: 10.1007/s004450050190

Fouquet Y, von Stackelberg U, Charlou J L, et al. 1991. Hydrothermal activity in the Lau back-arc basin: sulfides and water chemistry. Geology, 19(4): 303–306, doi: 10.1130/0091-7613(1991)019<0303:HAITLB>2.3.CO;2

Frey F A, Coffin M F, Wallace P J, et al. 2000. Origin and evolution of a submarine large igneous province: the Kerguelen Plateau and Broken Ridge, southern Indian Ocean. Earth and Planetary Science Letters, 176(1): 73–89, doi: 10.1016/S0012-821X(99)00315-5

Frick C, Kent L E. 1984. Drift pumice in the Indian and South Atlantic oceans. South African Journal of Geology, 87(1): 19–33

Ginibre C, Wörner G, Kronz A. 2007. Crystal zoning as an archive for magma evolution. Elements, 3(4): 261–266, doi: 10.2113/gselements.3.4.261

Guo Kun, Zhai Shikui, Wang Xiaoyuan, et al. 2018. The dynamics of the southern Okinawa Trough magmatic system: New insights from the microanalysis of the An contents, trace element concentrations and Sr isotopic compositions of plagioclase hosted in basalts and silicic rocks. Chemical Geology, 497: 146–161, doi: 10.1016/j.chemgeo.2018.09.002

Halbach P, Koschinsky A, Seifert R, et al. 1989. Diffuse hydrothermal fluid activity, biological communities, and mineral formation in the North Fiji Basin (SW Pacific): Preliminary results of the R/V Sonne Cruise SO-134. Interridge News, 8: 38–44

Head J W III, Wilson L. 2003. Deep submarine pyroclastic eruptions: Theory and predicted landforms and deposits. Journal of Volcanology and Geothermal Research, 121(3–4): 155–193, doi: 10.1016/S0377-0273(02)00425-0

Hédervari P. 1982. A possible submarine volcano near the central part of Ninety-East Ridge, Indian Ocean. Journal of Volcanology and Geothermal Research, 13(3–4): 199–211, doi: 10.1016/0377-0273(82)90050-6

Hibbard M J. 1981. The magma mixing origin of mantled feldspars. Contributions to Mineralogy and Petrology, 76(2): 158–170, doi: 10.1007/BF00371956

Iyer S D. 1996. A study of the volcanics of the Central Indian Ocean Basin and their relationship to the ferromanganese deposits [dissertation]. Kolkata: Jadavpur University

Iyer S D, Amonkar A A, Das P. 2018. Genesis of Central Indian Ocean basin seamounts: morphological, petrological, and geochemical evidence. International Journal of Earth Sciences, 107(7): 2517–2538, doi: 10.1007/s00531-018-1612-z

Iyer S D, Banerjee R. 1998. Importance of plagioclase morphology and composition in magmagenesis of the Carlsberg Ridge basalts. Journal of Indian Geophysical Union, 1(2): 63–72

Iyer S D, Karisiddaiah S M. 1988. Morphology and petrography of pumice from the Central Indian Ocean Basin. Indian Journal of Marine Science, 17: 333–334

Iyer S D, Prasad M S, Gupta S M, et al. 1997. Evidence for recent hydrothermal activity in the Central Indian Basin. Deep-Sea Research Part I: Oceanographic Research Papers, 44(7): 1167–1184, doi: 10.1016/S0967-0637(97)00001-0

Iyer S D, Sudhakar M. 1993. Coexistence of pumice and manganese nodule fields—evidence for submarine silicic volcanism in the Central Indian Basin. Deep-Sea Research Part I: Oceanographic Research Papers, 40(5): 1123–1129, doi: 10.1016/0967-0637(93)90092-H

Iyer S D, Sudhakar M. 1995. Evidences for a volcanic province in the Central Indian Basin. Journal of Geological Society of India, 46: 353–358

Kalangutkar N G. 2012. Petrology and petrogenesis of pumice from Central Indian Ocean Basin [dissertation]. Goa: Goa University

Kalangutkar N G, Iyer S D. 2012. Submarine silicic volcanism: Processes and products. Geo-Spectrum Interface, 6(1): 30–39

Kalangutkar N G, Iyer S D, Ilangovan D. 2011. Physical properties, morphology and petrological characteristics of pumices from the Central Indian Ocean Basin. Acta Geologica Sinica, 85(4): 826–839, doi: 10.1111/j.1755-6724.2011.00488.x

Kalangutkar N G, Iyer S D, Mascarenhas-Pereira M B L, et al. 2015. Hydrothermal signature in ferromanganese oxide coatings on pumice from the Central Indian Ocean Basin. Geo-Marine Letters, 35(3): 221–235, doi: 10.1007/s00367-015-0402-x

Kano K. 2003. Subaqueous pumice eruptions and their products: A review. In: White J D L, Smellie J L, Clague D A, eds. Explosive Subaqueous Volcanism. Geophysical Monograph Series. Washington, DC: American Geophysical Union, 140: 213–229

Kato Y. 1987. Woody pumice generated with submarine eruption. Journal of Geological Society of Japan, 93(1): 11–20

Kidd R B, Ramsay A T S, Sykes T J S, et al. 1992. An Indian Ocean framework for paleoceanographic synthesis based on DSDP and ODP results. In: Duncan R A, Rea D K, Kidd R B, et al., eds.

Synthesis of Results from Scientific Drilling in the Indian Ocean. Geophysical Monograph Series. Washington, DC: American Geophysical Union, 70: 403–422, doi: 10.1029/GM070p0403

Kimura S, Muan A. 1971. Phase relations in the system CaO-iron oxide-TiO2 in air. American Mineralogist: Journal of Earth and Planetary Materials, 56(7–8), 1332–1346

Kodagali V N. 1998. A pair of seamount chains in the Central Indian Basin, identified from multibeam mapping. Marine Geodesy, 21(2): 147–158, doi: 10.1080/01490419809388130

Kokelaar P, Busby C. 1992. Subaqueous explosive eruption and welding of pyroclastic deposits. Science, 257(5067): 196–201, doi: 10.1126/science.257.5067.196

Lonsdale P, Hawkins J. 1985. Silicic volcanism at an off-axis geothermal field in the Mariana Trough back-arc basin. Geological Society of American Bulletin, 96(7): 940–951, doi: 10.1130/0016-7606(1985)96<940:SVAAOG>2.0.CO;2

Martín-Barajas A, Lallier-Verges E. 1993. Ash layers and pumice in the Central Indian Basin: relationship to the formation of manganese nodules. Marine Geology, 115(3–4): 307–329, doi: 10.1016/0025-3227(93)90058-4

Mascarenhas-Pereira M B L, Nath B N, Borole D V, et al. 2006. Nature, source and composition of volcanic ash in sediments from a fracture zone trace of Rodriguez Triple Junction in the Central Indian Basin. Marine Geology, 229(1–2): 79–90, doi: 10.1016/j.margeo.2006.02.002

Mudholkar A, Fujii T. 1995. Fresh pumice from the Central Indian Basin: A Krakatau 1883 signature. Marine Geology, 125(1–2): 143–151, doi: 10.1016/0025-3227(95)00027-V

Mueller W, White J D L. 1992. Felsic fire-fountaining beneath Archean seas: Pyroclastic deposits of the 2730 Ma Hunter Mine Group, Quebec, Canada. Journal of Volcanology and Geothermal Research, 54(1–2): 117–134, doi: 10.1016/0377-0273(92)90118-W

Mukherjee A D, Iyer S D. 1999. Synthesis of morphotectonics and volcanics of the Central Indian Ocean Basin. Current Science, 76(3): 296–304

Mukhopadhyay R, Ghosh A K, Iyer S D. 2018. The Indian Ocean Nodule Field: Geology and Resource Potential. 2nd ed. Amsterdam: Elsevier

Müller A, Breiter K, Seltmann R, et al. 2005. Quartz and feldspar zoning in the eastern Erzgebirge Volcano–Plutonic Complex (Germany, Czech Republic): evidence of multiple magma mixing. Lithos, 80(1–4): 201–227, doi: 10.1016/j.lithos.2004.05.011

Neumann von Padang M. 1967. Catalogue of active volcanoes of the world part xxi Atlantic Ocean. Roma: International Association of Volcanology, 128

Oba N, Tomita K, Yamamoto M, et al. 1983. Geochemical study of volcanic products, in particular to pumice flow, of the Krakatau Group, Indonesia. Reports of the Faculty of Science, Kagoshima University (Earth Sciences and Biology), (16): 21–41

Pal T, Mitra S K, Sengupta S, et al. 2007. Dacite–andesites of Narcondam volcano in the Andaman Sea—an imprint of magma mixing in the inner arc of the Andaman–Java subduction system. Journal of Volcanology and Geothermal Research, 168(1–4): 93–113, doi: 10.1016/j.jvolgeores.2007.08.005

Pattan J N, Mudholkar A V, Jai Sankar S, et al. 2008. Drift pumice in the Central Indian Ocean Basin: Geochemical evidence. Deep-Sea Research Part I: Oceanographic Research Papers, 55(3): 369–378, doi: 10.1016/j.dsr.2007.12.005

Pattan J N, Parthiban G, Moraes C, et al. 2016. A note on chemical composition and origin of ferromanganese oxide coated and uncoated pumice samples from Central Indian Ocean Basin. Journal of the Geological Society of India, 87(1): 62–68, doi: 10.1007/s12594-016-0374-0

Pattan J N, Pearce N J G, Parthiban G, et al. 2013. The origin of ferromanganese oxide coated pumice from the Central Indian Ocean Basin. Quaternary International, 313–314: 230–239, doi: 10.1016/j.quaint.2013.07.128

Poulsen H F, Neuefeind J, Neumann H B, et al. 1995. Amorphous silica studied by high energy X-ray diffraction. Journal of Non-Crystalline Solids, 188(1–2): 63–74, doi: 10.1016/0022-3093(95)00095-X

Ray J S, Pande K, Awasthi N. 2013. A minimum age for the active Barren Island volcano, Andaman Sea. Current Science, 104(7): 934–939

Ray D, Rajan S, Ravindra R, et al. 2011. Microtextural and mineral chemical analyses of andesite–dacite from Barren and Narcondam islands: Evidences for magma mixing and petrological implications. Journal of Earth System Science, 120(1): 145–155, doi: 10.1007/s12040-011-0006-4

Risso C, Scasso R A, Aparicio A. 2002. Presence of large pumice blocks on Tierra del Fuego and South Shetland Islands shorelines, from 1962 South Sandwich Islands eruption. Marine Geology, 186(3–4): 413–422, doi: 10.1016/S0025-3227(02)00190-1

Schott F, McCreary J P. 2001. The monsoon circulation of the Indian Ocean. Progress in Oceanography, 51: 1–123, doi: 10.1016/S0079-6611(01)00083-0

Shinjo R, Kato Y. 2000. Geochemical constraints on the origin of bimodal magmatism at the Okinawa Trough, an incipient back-arc basin. Lithos, 54(3–4): 117–137, doi: 10.1016/S0024-4937(00)00034-7

Sigurdsson H, Sparks R S J, Carey S N, et al. 1980. Volcanogenic sedimentation in the Lesser Antilles Arc. The Journal of Geology, 88(5): 523–540, doi: 10.1086/628542

Sukumaran N P, Banerjee R, Borole D V, et al. 1998. Some aspects of volcanic ash layers in the Central Indian Basin. Geo-Marine Letters, 18(3): 203–208, doi: 10.1007/s003670050069

Svalnov V N. 1981. The effect of island volcanism in the Indian Ocean. Oceanology, 21: 606–612

Vance J A. 1965. Zoning in igneous plagioclase: patchy zoning. The Journal of Geology, 73(4): 636–651, doi: 10.1086/627099

Whitham A G, Sparks R S J. 1986. Pumice. Bulletin of Volcanology, 48(4): 209–223, doi: 10.1007/bf01087675

Wilson C J N, Blake S, Charlier B L A, et al. 2006. The 26.5 ka Oruanui Eruption, Taupo Volcano, New Zealand: Development, characteristics and evacuation of a large rhyolitic magma body. Journal of Petrology, 47(1): 35–69, doi: 10.1093/petrology/egi066